3062 *Macromolecules* **1998,** *31,* 3062−3074

Thermodynamics of Amorphous Starch−Water Systems.
2. Concentration Fluctuations

D. Benczédi,[†] I. Tomka,* and F. Escher

Institute of Polymers, Institute of Food Science, Swiss Federal Institute of Technology ETH,
8092 Zurich, Switzerland

Received July 1, 1996; Revised Manuscript Received November 3, 1997

ABSTRACT: This paper presents a theoretical and experimental study of the sigmoidal water sorption isotherms of amorphous starch. Sorption isotherms have been measured by gas chromatography at infinite dilution of water in starch and by isothermal and isosteric sorption experiments in an extended concentration and temperature range in which the biopolymer behaves either as a brittle glass or as a rubbery melt. A maximum value of the isothermal activity coefficient of water is observed at a composition corresponding to the glass transitions measured by calorimetry. Therefore, the partial derivatives of the activity coefficient of water with respect to concentration and temperature are positive in glasses and negative in melts. A transition from sigmoidal to Flory type sorption is estimated to occur at 175 °C, which is lower than the glass transition of dry starch. The distribution of water molecules in glasses and melts is analyzed with the Kirkwood theory of solutions. In glasses, water shows large negative excluded volumes typical of an antiplasticizer, as reflected also in the density increase observed at low water concentrations. In melts, water shows positive excluded volumes typical of a plasticizer having recovered its motional freedom restricted in the glassy state. Up to 80 °C, the self-clustering functions of water in melts diverge at higher water contents. These functions only take finite values above this temperature once a full melting of the starch−starch hydrogen bond interaction has occurred. The sigmoidal water sorption isotherms are analyzed with a new explicit relationship combining the generalized Freundlich adsorption model and the Flory model of polymer solutions. A restricted translational and rotational freedom is predicted for the adsorption water, and a clustering tendency is predicted for the solution water. The Freundlich−Flory sorption model provides a consistent description of the solvation, the swelling, and the dissolution of hydrophilic polymer glasses in a solvent like water whereas the Brunauer−Emmet−Teller model is only physically meaningful for the adsorption of nonsolvents such as oxygen or nitrogen gases.

Introduction

The term sorption is used to describe gas or solvent uptake by adsorption on surfaces or at specific molecular sites and by swelling due to the formation of solvent clusters in a polymer matrix. Early works on the investigation of the surface area of proteins have shown that the adsorption of nonpolar gases such as nitrogen or oxygen takes place at the surface whereas the sorption of polar gases such as water or ammonia takes place by swelling and involves the solvation of specific polar groups.[1−4] Depending upon the entropies and enthalpies of mixing, different modes of sorption can be distinguished.[5,6]

The sorption of a weakly interacting gas in a rubbery polymer is described by Henry's law. If the polymer is glassy, the adsorption of a weakly interacting gas is larger at low pressures than according to Henry's law and it is described by a combination of the Langmuir and the Henry isotherms.[5−9] As the affinity of the solvent for itself and for the polymer increases, a macroscopic swelling of the polymer occurs during sorption as described by the Flory theory of athermal or endothermic polymer solutions.[10−13]

The combinatorial entropy of mixing arising from the athermal dilution of a polymer in its monomeric analogues can be calculated by considering the polymer as composed of a number r of mers, each mer occupying one site on a three-dimensional quasi-lattice.[10−13] The activity coefficient, γ_1, of a solvent is then related to the volume fraction, φ_2, of the polymer in the mixture by

$$\gamma_1 = \left(1 - \frac{2}{z}\varphi_2\right)^{-z/2} \tag{1}$$

which gives in the limit of an infinitely large coordination number, z,

$$\gamma_1 = \exp(\varphi_2 + \chi^\infty \varphi_2^{\,2}) \tag{2}$$

where χ^∞ is a temperature dependent, but concentration independent, van Laar heat of mixing related to the change in the potential energy of a solvent molecule as it is transferred from the pure solvent to the pure polymer. The exponent ∞ denotes the infinite dilution of the solvent in the polymer ($\varphi_1 \rightarrow 0$).[25,26]

The Flory model in eq 2 predicts the exponential sorption isotherms of athermal ($\chi^\infty = 0$) or endothermic ($\chi^\infty > 0$) mixtures. The experimental value of χ^∞ is of 0.4 for a typically apolar mixture of benzene in rubber at 25 °C, whereas it is of 0.2 according eq 1 for $z = 6$ and of 0 according to eq 2 for $z \rightarrow \infty$.[27] In a good solvent, the interaction between two macromolecules is weaker than the interaction of the solvent with the macromolecule and $\chi^\infty < 0.5$, whereas the opposite is true in a poor solvent in which a partial association of the macromolecule persists and $\chi^\infty > 0.5$.[10−13]

When the polymer−solvent mixing is exothermic at the limit of zero solvent concentration ($\chi^\infty < 0$), the

---

* Corresponding author.

[†] Current address: Firmenich Inc., R&D Division, 1211 Geneva 8, Switzerland.

S0024-9297(96)00950-3 CCC: $15.00

sorption isotherms deviate from the exponential Flory reference isotherm due to an overproportional increase of the solvent concentration with the solvent activity at low solvent concentrations. Such isotherms are sigmoidal and are therefore characterized by $\chi^\infty < 0$ as well as by a clearly composition dependent χ parameter, which is negative at low solvent concentrations and positive at higher ones. Sigmoidal water sorption isotherms were reported for collagen,[27] casein,[20,21] various types of starches and numerous other biopolymers,[14] which can be brought through their glass transition point isothermally by water uptake. The same sorption isotherms have also been observed with synthetic polymers such as nylon, cellulose nitrate and ethylcellulose,[28] alkanols in water,[29] vinyl chloride in poly(vinyl chloride),[30] and chloroform in poly(propylene oxide).[31] A density increase observed previously at low water concentrations in polymer glasses such as starch or ethylcellulose has been shown to disappear as these polymers are brought toward their glass transition by plasticization and as their water sorption isotherm changes from sigmoidal to Flory type.[38,63–65]

The Brunnauer–Emmet–Teller multilayer adsorption model[1] is frequently used to analyze sigmoidal sorption isotherms.[6] As shown previously, the surface areas derived for proteins are only physically meaningful when they are derived from the sorption isotherms of nonsolvents such as nitrogen or oxygen gases as opposed to solvents such as water and ammonia vapors.[2–4] This means that solvents find their way in amorphous polymers by disrupting polymer–polymer interactions, and their sorption at equilibrium is therefore an invariant of the sample preparation whereas the sorption of a nonsolvent depends on the specific surface area of the sample.

The solvation of specific polar groups by water is known to cause a distribution of adsorption energies, as reflected in a Freundlich type adsoption in which the Langmuir case is the limiting one for constant adsorption energies.[2–4,14–21] A new explicit model[22] combining a Flory and a generalized Freundlich isotherm is presented below and used to analyze sorption of water in amorphous potato starch glasses and melts.[22] The Kirkwood theory of solutions is used to analyze the distribution of water in starch with a particular emphasis on its role as an antiplasticizer.[23,24,38,63–66]

Theory

Freundlich–Flory Model of Sorption. Polymer solvent mixtures undergoing a glass transition upon solvent uptake have their sorption isotherms crossing over and losing their sigmoidal shape as an increase in temperature shifts their glass transition point toward lower solvent contents (see Figure 3). The restricted configurational rearrangements of polymers in the glassy state do not allow us to calculate the combinatorial entropy of mixing with the Flory model of polymer solutions. We assume, therefore, that a second sorption mechanism takes place simultaneously during the isothermal dilution of partially frozen systems.

From a macroscopic point of view, water uptake by hydrophilic polymer glasses is analogous to a hole-filling process, as reflected by increased densities and by Freundlich adsorption modes at low water concentrations.[2–4,22,38,63–65] To predict the resulting sigmoidal sorption isotherms, the generalized Freundlich model of adsorption and the Flory model of polymer solutions are combined into an explicit relationship. It is assumed that the two coexisting mixed solvent phases described by this combined sorption model have equal thermodynamic activity at equilibrium.[22] Using the volume fractions, φ, to denote the relative concentration of each of the two phases composing the solvent (index 1) sorbed at equilibrium by a polymer (index 2), we have

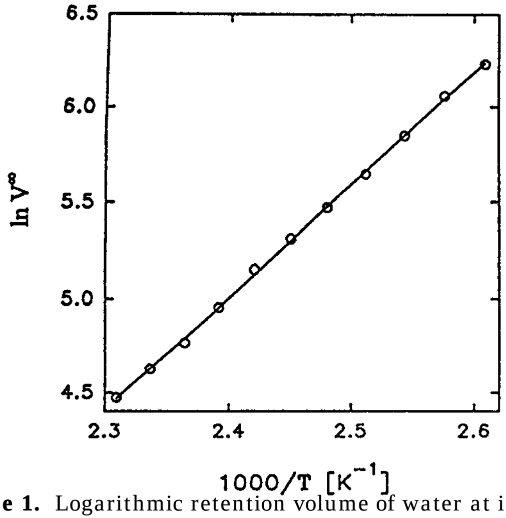

Figure 1. Logarithmic retention volume of water at infinite dilution in amorphous starch, V^∞, as a function of temperature. The heat of activation obtained from the slope is used to calculate the partial molar excess heat of mixing of water at infinite dilution.

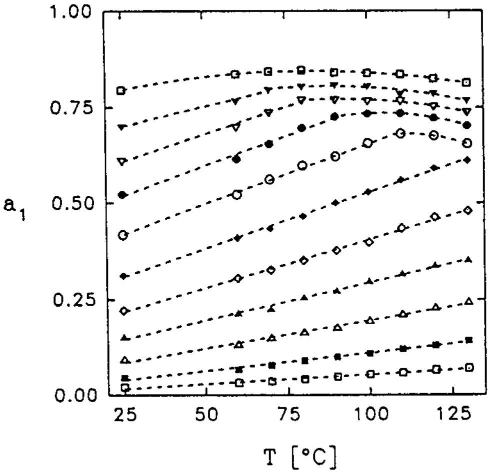

Figure 2. Isosteres combining the results obtained at 25, 60, 70, 80, 90, 100, 110, 120, and 130 °C with samples containing from the bottom to the top 0.023, 0.035, 0.049, 0.062, 0.076, 0.092, 0.106, 0.122, 0.137, 0.153, and 0.176 weight fraction of water.

$$\varphi_1 + \varphi_2 = \varphi_1^{\mathrm{Fr}} + \varphi_1^{\mathrm{Fl}} + \varphi_2 = 1 \tag{3}$$

where the indices Fr and Fl denote solvent molecules involved in Freundlich and Flory type sorption, respectively.

The adsorption isotherm obtained on defining $N^0(\epsilon)\,\mathrm{d}\epsilon$ as the number of sites whose adsorption energy lies between ϵ and $\epsilon + \mathrm{d}\epsilon$, is[17–21]

$$\frac{N}{N^0}(p) = \int_0^\infty \frac{N^0(\epsilon)\,\mathrm{d}\epsilon}{1 + 1/(a_1 q)\exp\{-\epsilon/kT\}} \tag{4}$$

where N is the number of solvent molecules adsorbed at pressure p and temperature T, k is the Boltzmann

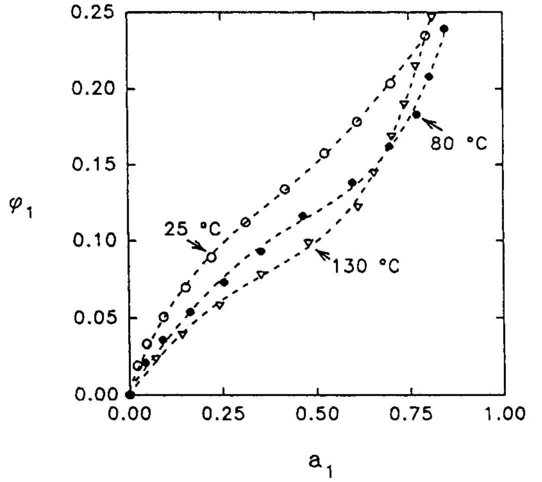

Figure 3. Water sorption isotherm of amorphous starch at 25, 80, and 130 °C. a_1 is water activity, and φ_1 is the volume fraction of water in amorphous starch.

constant, and q is the mean molecular partition function of the adsorbed molecules (see also Appendix I). The simplest isotherm corresponding to eq 4 is (see also Appendix I)[17,18]

$$\frac{\varphi_1^{\mathrm{Fr}}}{\varphi_2} = \theta^0\left(\frac{a_1}{a_1 + 1/q}\right)^f \tag{5}$$

where $\varphi_1^{\mathrm{Fr}}/\varphi_2$ is the equilibrium ratio of volume fractions of adsorbed solvent to adsorbing polymer corresponding to a thermodynamic solvent activity of a_1. θ^0 is the same ratio at saturated vapor pressure ($a_1 = 1$) of the solvent, $(\varphi_1^{\mathrm{Fr}}/\varphi_2)^0$. The parameter f reflects the heterogeneity of the adsorption energies and the equation is physically meaningful for $0 < f < 1$, where the distribution of the adsorption energies is close to Gaussian.[17,18] The Langmuir equation is recovered when $f = 1$, as then all the adsorption energies are the same.

Considering that φ_1^{Fl} is sorbed by a solid mixture of φ_1^{Fr} and φ_2, the free energy of mixing $\Delta G_{\mathrm{m}}^{\mathrm{Fl}}$ according to the Flory model of polymer solutions is[10,11]

$$\Delta G\mathrm{m}^{\mathrm{Fl}} = N_1^{\mathrm{Fl}} \ln \varphi_1^{\mathrm{Fl}} + (N_1^{\mathrm{Fr}} + \mathrm{N}_2) \ln(\varphi_1^{\mathrm{Fr}} + \varphi_2) + \varphi_1^{\mathrm{Fl}}(\varphi_1^{\mathrm{Fr}} + \varphi_2)\chi^{\infty} \tag{6}$$

where χ^{∞} represents the change in the potential energy of a solvent molecule N_1^{Fl} as it is transferred from the pure solvent into the solid mixture composed of the polymer N_2 and of the adsorbed solvent N_1^{Fr} (see also Appendix II). The corresponding Flory isotherm is

$$a_1 = \varphi_1^{\mathrm{Fl}} \exp[(1 - \varphi_1^{\mathrm{Fl}}) + \chi^{\infty}(1 - \varphi_1^{\mathrm{Fl}})^2] \tag{7}$$

The equal thermodynamic activity of the solvent in the two phases being the same at equilibrium, eq 3 combines eqs 5 and 7 into an explicit analytical description of the solvent uptake with four adjustable parameters (f, q, θ^0, χ^{∞}). The one-parameter Flory isotherm is recovered in the limiting case where the contribution of Freundlich adsorption becomes negligible ($\varphi_1^{\mathrm{Fr}} \to 0$).[22]

Kirkwood Theory of Solutions. Kirkwood and Buff[23] have shown that there are exact relationships between integrals of molecular radial pair correlation functions and concentration derivatives of volume, pressure, and chemical potential. The cross fluctuations in the number of molecules of species i and j can be related to the volume integral G_{ij} of a spatial distribution function, $g_{ij}(R)$, which depends only on the scalar distance, R, between centers of mass of ij pairs.

$$\frac{G_{ij}}{V} = \frac{1}{V}\int_0^{\infty}[g_{ij}(R) - 1]\, 4\pi R^2\, \mathrm{d}R = \left[\frac{\langle N_i - N_j\rangle - \langle N_i\rangle\langle N_j\rangle}{\langle N_i\rangle\langle N_j\rangle} - \frac{\delta_{ij}}{N_i}\right] \tag{8}$$

In eq 8, $\langle ... \rangle$ stands for an average in the grand canonical ensemble, V is a convenient reference volume, N is the number of molecules of species i and j, and δ_{ij}, is the Kronecker delta. Since no assumption as to the form of the intermolecular potential energy is invoked in the derivation, this equation is free of explicit interaction terms and does not depend on the particular chemical structure or on the size of the molecules. In this way, g_{ij} can be interpreted as the integral of a more general pair correlation function over all relative orientations of the pairs, containing implicitly the effects of internal and external degrees of freedom of the molecules in the system. The clustering function concept is a powerful tool to study molecular distributions in hydrogen-bonded systems.

Using the Gibbs–Duhem equation, on a volume fraction scale, the self-clustering function of a solvent,

$$\frac{\varphi_1}{\bar{v}_1}\frac{\partial \gamma_1}{\partial a_1} + \frac{\varphi_2}{\bar{v}_2}\frac{\partial \gamma_2}{\partial a_2} = 0 \tag{9}$$

G_{11}/v_1, can be related to the partial derivatives appearing in eq 8.[24,32] On solving for the G_{ij} in the eqs system eqs 17, 18, and 21 of Kirkwood's original paper,[23] one is left with a total of three clustering functions. For condensed systems having a negligible compressibility, κ ($\kappa RT \ll G_{ij}$), the three reduced volume integrals can be written

$$\frac{G_{11}}{\bar{v}_1} = -\varphi_2\left(\frac{\partial \gamma_1}{\partial a_1}\right)_{P,T} - 1 \tag{10}$$

$$\frac{G_{22}}{\bar{v}_2} = -\frac{\bar{v}_1}{\bar{v}_2}\frac{\varphi_1}{\varphi_2}\left(\frac{\partial \gamma_1}{\partial a_1}\right)_{P,T} - 1 \tag{11}$$

$$\frac{G_{12}}{\bar{v}_1} = \frac{G_{21}}{\bar{v}_2} = \varphi_1\left(\frac{\partial \gamma_1}{\partial a_1}\right)_{P,T} - 1 \tag{12}$$

Since G_{ij} itself is not symmetrical to an interchange of the indices for molecules differing in size ($G_{ij} \neq G_{ji}$), it is important to assess clearly the role of the indices in eq 12. In the following, we consider that g_{ij} in eq 8 determines the average density of molecules of species i in a given configuration with respect to a molecule of species j. G_{12} is thus an expression for the volume excluded by a solvent molecule positioned next to the repeating unit of a polymer and G_{21} describes the volume excluded by repeating polymer units positioned next to a solvent molecule. In this way, the two cluster integrals appearing in eq 12 are only symmetrical to an interchange of the indices in their reduced form so that $G_{12}/\bar{v}_1 = G_{21}/\bar{v}_2$.[22] Since $(\partial\gamma_1/\partial a_1) = 0$ in mixtures obeying Raoult's law, eq 10 indicates that every molecule excludes exactly its own volume to the other molecules ($G_{11}/\bar{v}_1 = -1$) in an ideal mixture as in the pure state. Furthermore, $G_{11}/\bar{v} < -1$ indicates a preferential heterocoordination of the solvent with the polymer, while $G_{11}/\bar{v}_1 > -1$ indicates a preferential homocoordination of the solvent.

The cluster integrals can also be evaluated from X-ray- and neutron-scattering experiments. The scattering intensity of a binary mixture can be related to three structure factors constructed from the Fourier transforms of the local number density and local concentration.[33] The three structure factors represent the mean-square fluctuations in the particle number, in the concentration, and in the average of the correlation between the two fluctuations, respectively. With the partial derivative introduced in eqs 10−12, the volume fraction-related concentration−concentration correlation $S^{\varphi}_{\mathrm{CC}}(0)$ can be written[34,35]

$$\frac{S^{\varphi}_{\mathrm{CC}}(0)}{\bar{v}_1} = \frac{RT}{\bar{v}_1}\left(\frac{\partial g_1^{2\varphi}}{\partial {\varphi_1}^2}\right)_{P,T}^{-1} = {\varphi_1}^2\varphi_2\left(\frac{\partial \gamma_1}{\partial a_1}\right)_{P,T} \tag{13}$$

where g^{φ} is the volume fraction-related intensive Gibbs free energy.[36] For a mixture obeying Raoult's law, $\tilde{S}^{\varphi}_{\mathrm{CC}}(0) = S^{\varphi}_{\mathrm{CC}}(0)/\bar{v}_1 = \varphi_1\varphi_2$ since then $\gamma_1 = 1$ and $\partial\varphi/\partial a_1 = 1$. The results of scattering experiments at small angles can also be related to the concentration dependent χ parameter by the following equation[34−38]

$$\tilde{S}^{\varphi}_{\mathrm{CC}}(0) = \left[\frac{1}{\varphi_1} + \frac{1}{\bar{v}_2\varphi_2} - \frac{1}{\varphi_2}\frac{\partial({\varphi_2}^2\chi)}{\partial\varphi_2}\right]^{-1} \tag{14}$$

The clustering functions can thus be calculated from either eq 13 or eq 14.

Experimental Section

The amorphous polymer used in the present investigations was obtained by the extrusion of potato starch with water. The equation of state properties of this system have been described previously,[22,38] while the vapor pressure isotherms of this material are presented here. These were obtained by combining the results of gravimetric, manometric, and chromatographic measurements covering the concentration range extending from dry starch to a system of starch containing 17.5 wt % water.

Gas Chromatography at Infinite Dilution. The activity coefficient of water at infinite dilution in starch was measured between 105 and 165 °C by gas chromatography using a method developed by Guillet and co-workers.[39,40] The chromatography columns consisted of copper tubing, of 5 mm inner diameter, packed with Chromosorb T (Teflon) containing about 4 wt % dry amorphous starch (stationary phase). To avoid diffusion-controlled sorption and to obtain retention times independent of the flow rate, the specific surface area of the samples had to be increased by preparing an aqueous solution containing 2 wt % amorphous starch powder ($\varnothing < 50\ \mu$m) followed by removal of the water by freeze-drying. During the experiments, the column was immersed in an oil bath thermostated to ±0.1 °C. High-purity helium was used as the carrier gas and retention times were measured using a catharometer. The void volume of the packed columns was determined with 3 μL of air.

In gas chromatography, the fundamental experimental quantity is the specific retention volume, V^{∞}, of the volatile compound, which is defined as

$$V^{\infty} = F\frac{(t_{\mathrm{w}} - t_{\mathrm{a}})}{w} \tag{15}$$

where t_{a} and t_{w} are the retention times of a noninteracting marker (air) and of water, respectively, while w is the weight of starch in the column. The experimental flow rate, F', at temperature T_{F} is corrected to standard temperature and pressure, p_{o}, with the following equation

$$F = F'\left(\frac{273.15}{T_{\mathrm{F}}}\right)\left(\frac{760}{p^0}\right)\left(\frac{p_{\mathrm{o}} - p_{\mathrm{w}}}{p_{\mathrm{o}}}\right)\frac{3}{2}\left[\frac{(p_{\mathrm{i}}/p_{\mathrm{o}})^2 - 1}{(p_{\mathrm{i}}/p_{\mathrm{o}})^3 - 1}\right] \tag{16}$$

In eq 16, the third factor corrects for the vapor pressure, p_{w}, of water in the flow meter, the fourth factor corrects the flow rate for the compressibility of the carrier gas in the column, and p_{i} is the pressure at the inlet of the column.[41]

The heat of evaporation can be estimated from the slope of ln V^{∞} vs ($1/T$) and can be used to calculate the partial molar excess heat of mixing of water at infinite dilution in starch, $(\Delta H_1^{\mathrm{E}})^{\infty}$, when the enthalpy of vaporization, ΔH_{v}^0, is known.

$$(\Delta H_1^{\mathrm{E}})^{\infty} = \Delta H_{\mathrm{v}}^0 - R\frac{\partial \ln(V_{\mathrm{g}}^0)}{\partial(1/T)} \tag{17}$$

The limiting behavior of ${\gamma_1}^{\infty}$ and of χ^{∞} can be calculated from the following relationship

$$\ln {\gamma_1}^{\infty} = -\frac{\rho_1}{\rho_2}\left\{\ln\left(\frac{273.15R}{p^0 M_1 V_{\mathrm{g}}^0}\right) + \left[\frac{p^0(B_{11} - V_1)}{RT}\right]\right\} = \chi^{\infty} + 1 \tag{18}$$

where M_1, V_1, p^0, and B_{11} are the molecular weight, the molar volume, the saturation vapor pressure, and the second virial coefficient of water at the column temperature, R is the gas constant, and ρ_1 and ρ_2 are the specific densities of pure water and pure starch, respectivey.[25,26,42]

Isothermal and Isosteric Sorption at Finite Concentrations. The equilibrium vapor pressure properties of water in amorphous starch were studied at 25 °C with the isothermal sorption technique reviewed in detail elsewhere.[43] The moisture content of starch powder ($f < 0.5$ mm) previously dried at 80 °C was established by equilibrating the samples at 25 ± 0.1 °C above aqueous sulfuric acid solutions. The diffusion coefficient of water in starch is known to increase logarithmically with the water content and to reach the self-diffusion value of pure water only at higher water contents.[44,45] The concentration of the acid solutions was estimated from the results of three titrations (1 N NaOH titrisol, Fluka AG, Switzerland) that lay within 1% of each other.

At higher temperatures, the activity coefficient of water in starch was obtained by measuring the isosteric partial pressure of water in amorphous starch between 60 and 130 °C. The capacitive manometer used (Henni AG, Switzerland) had a sensitivity of ±1 mbar and a full scale of 3 bar. The manometer cell was placed in an air thermostat controlled to within ±0.1 °C. The temperature in the manometer cell itself was controlled by a proportional-differential-integral temperature monitor equipped with a PT 1000 thermocouple, and the temperature of the samples was kept within ±0.01 °C of the selected value. A sample of 5 g of amorphous starch powder of known water content was sealed tightly in the manometer cell using silvered chrome nickel O-rings with combined plastic and elastic deformational properties (Prophysik AG, Vaduz, Lichtenstein). The variation of the sample concentration is kept within ±0.01 between 25 and 130 °C if the unoccupied volume fraction of the sample cell is kept below 0.2.

The gas phase enclosed in the manometer cell was composed of water vapor above the sample with a partial pressure $p(T_0) = a(T_0)\,p^0(T_0)$, where p^0 was the saturation vapor pressure of water at temperature T_0, and of the pressure of air $p_{\mathrm{a}}(T_0)$ enclosed at atmospheric pressure $p_{\mathrm{atm}}(T_0) = p_{\mathrm{a}}(T_0) + p(\mathrm{T}_0)$. The density of the air enclosed was estimated with a mercury barometer ($\rho = p_a\ (T_0)/RT_0$) and was used to calculate the corresponding pressure at temperature T, ($p_a(T) = RT/\rho$). The zero pressure reading of the manometer, $p_0(T)$, was calibrated with dry starch ($w_1 > 0.001$) at any experimental temperature and the partial pressure of water at a given temperature, $p(T)$, was calculated from the experimental pressure, $p_{\exp}(T)$, using $p(T) = p_{\exp}(T) - p_a(T) - p_0(T)$. The volume fraction related activity coefficient of water in starch, γ_1, is calculated from the partial and saturation pressures of water, p, and p^0, and the second virial coefficient of water, B_{11}, with

$$\gamma_1 = \frac{a_1}{\varphi_1} = \frac{1}{\varphi_1}\frac{p}{p^0}\exp\left[-\frac{B_{11}(p^0 - p)}{RT}\right] \tag{19}$$

Estimation of the Solubility Parameter. The solubility parameter, δ_1, of a solvent, derived originally by Scatchard and Hildebrand for regular solutions,[14] is defined as the square root of the cohesive energy density, which is the ratio of the energy of vaporization, E_1^V, to the molar volume, V_1.

$$\delta_1 = \left(\frac{E_1^{\ V}}{V_1}\right)^{1/2} = \left(\frac{H_1^{\ V} - RT}{V_1}\right)^{1/2} \tag{20}$$

$$\frac{\chi^\infty}{V_1} = \frac{(\delta_1 - \delta_2)^2}{RT} \tag{21}$$

χ^∞ is related to the work required to remove a water molecule from starch at infinite dilution, i.e., in the absence of water–water interactions. Previous work has shown that the solubility parameter, δ_2, of the nonvolatile polymer component is generally approximated by combining the Scatchard–Hildebrand and Flory approaches.[46] Using eq 21, $\delta_1^2/RT - \chi^\infty/V_1$ is plotted as a function of δ_1 to obtain a line with slope $2\delta_2/RT$. In this way the solubility parameter, δ_2, of the nonvolatile component can be estimated when δ_1 and χ^∞ are known for several solvents in the same polymer. δ can therefore also be estimated for mixtures from the temperature dependence of χ with the physically meaningful solution of eq 21, which is[22]

$$\delta = \delta_1 - \left[\left(4R\frac{\partial(\chi/V_1)}{\partial(1/T)}\right)^{1/2}\right]/2 \tag{22}$$

Results

The strong hydrogen bonding of water with itself and with starch limited the sorption experiment by gas chromatography to temperatures above 105 °C if retention times are kept smaller than 15 min and at flow rates of 0.1–0.2 mL/s. The sample size was kept below 0.03 μL to ensure that water–water interactions could be neglected during the experiment. With these conditions, the elution peaks produced by the chromatograph were symmetrical, as they must be for equilibrium sorption.

The specific retention volumes, V^∞, of water at infinite dilution in amorphous starch were measured at 5 °C intervals at temperatures ranging from 110 to 160 °C. The results are presented in Table 1 while Figure 1 shows the fit of ln $V^\infty(1/T)$ to the linear equation ln $V^\infty(1/T) = -9.129 + 5889(1/T)$. The regression coefficient of 0.9997 corresponds to an experimental uncertainty of 1–3% in the retention volumes, which is typical for such experiments.[37] The value estimated for $(\Delta H_1^E)^\infty$, −12.7 kJ/mol, corresponds well with the literature value obtained for dry native potato starch by immersion calorimetry, −12.54 kJ/mol.[14]

The sorption isotherm at 25 °C presented in Table 2 was obtained from the average of three values within an experimental uncertainty of ±0.5% in the activity, which corresponds to a variations of ±0.1 °C in the temperature during the experiment.[43] A comparison with the sorption isotherm of native potato starch[15] shows that the semicrystalline biological structure swells somewhat more than the processed amorphous material. At temperatures ranging from 60 to 130 °C, the partial pressure, p, of water in amorphous starch was measured by increasing the temperature of samples in 10 °C steps. With the temperature controlled to ±0.01 °C during the measurements, the experimental accuracy was mainly limited by the manometer having a sensitivity of ±1 mbar. At 60 °C, this sensitivity value represents 5–10% of the measured vapor pressure, while it represent about 1% at the highest temperatures.

Table 1. Specific Retention Volume of Water in Amorphous Starch at Zero Water Concentration, V^∞, the Volume Fraction Related Activity Coefficient, γ^∞ and Flory Interaction Parameter, χ^∞, the Saturation Pressure, p^0, and the Second Virial Coefficient, B_{11}, of Water as a Function of Temperature (*Handbook of Physics and Chemistry*, 1982)

T (°C)	p^0 (bar)	B_{11} (L/mol)	V^∞ (cm^3/g)	γ^∞	χ^∞
25.00	0.0322	−1.158	41050	0.522	−1.650
60.00	0.1992	−0.718	5154	0.883	−1.124
70.00	0.3117	−0.636	3079	1.005	−0.995
80.00	0.4736	−0.567	1894	1.133	−0.875
90.00	0.7011	−0.509	1197	1.269	−0.762
100.00	1.0133	−0.459	774.8	1.412	−0.655
110.00	1.4326	−0.416	513.2	1.559	−0.556
120.00	1.9853	−0.379	347.2	1.712	−0.462
130.00	2.7012	−0.347	239.4	1.869	−0.374

The activity coefficient and the related concentration dependent Flory interchange parameters measured at 25 °C and between 60 and 130 °C are presented in Table 2. The isosteres of water in starch measured at finite concentrations are shown in Figure 2, where the temperature dependence of the activity of water is plotted at constant composition. It can be seen that, at the lowest water concentrations (corresponding to glasses), the activity of water has a simple, linear temperature dependence. Due to the melting of the samples as the water concentration and the temperature are increased, the activity of water is not further increased by an additional increase in the temperature. As a consequence of the melting, the powdery samples exhibiting deviations from the linear temperature dependence of the isosteric water activity were caked together at the end of the experiment. For the same reason, the corresponding sorption isotherms measured at different temperatures cross each other, as shown in Figure 3, at 25, 80, and 130 °C.

In Figure 4, activity coefficients are plotted as a function of the water activity at 25, 80, and 130 °C. It can be seen that the maximum value of the excess function, $\gamma_1(a_1)$, is shifted toward lower water activities as the experimental temperature is increased. A plot of χ as a function of the molar concentration of water in starch at the same three temperatures (Figure 5) reveals the same type of concentration behavior. It can be seen that the position of the maxima at 80 and 130 °C corresponds well with the glass-melt transition observed by calorimetry whereas higher water contents are needed to cause a transition at room temperature. It can also be seen that $\partial\gamma_1/\partial a_1$ and $\partial\gamma_1/\partial T$ are positive in glasses and negative in melts and that both $\gamma_1(a_1)$ and $\chi(x_1)$ become clearly discontinuous at the glass–melt transition on isotherms measured above 80 °C.

Table 2. Activity, a_1, and Activity Coefficient, γ_1, and Related Concentration Dependent χ Parameter for Amorphous Starch Containing w_1 and φ_1 Weight Fraction and Volume Fraction of Water, Respectively, at 25, 60, 70, 80, 90, 100, 110, 120, and 130 °C

w_1	x_1	φ_1	a_1	γ_1	χ	w_1	x_1	φ_1	a_1	γ_1	χ
					25 °C						
0.000	0.000	0.000	0.000	0.522	−1.650	0.106	0.517	0.135	0.418	3.125	0.365
0.023	0.175	0.019	0.021	1.077	−0.942	0.122	0.557	0.159	0.524	3.321	0.504
0.035	0.246	0.033	0.045	1.407	−0.669	0.137	0.587	0.180	0.611	3.422	0.606
0.049	0.315	0.051	0.093	1.823	−0.387	0.153	0.620	0.205	0.702	3.453	0.697
0.062	0.374	0.070	0.151	2.169	−0.180	0.176	0.657	0.236	0.796	3.391	0.778
0.076	0.425	0.090	0.221	2.485	−0.001	1.000	1.000	1.000	1.000	1.000	0.000
0.092	0.476	0.113	0.313	2.799	−0.179						
					60 °C						
0.000	0.000	0.000	0.000	0.883	−1.124	0.106	0.517	0.136	0.522	3.824	0.641
0.023	0.175	0.020	0.033	1.590	−0.537	0.122	0.557	0.160	0.616	3.842	0.718
0.035	0.246	0.035	0.068	1.953	−0.317	0.137	0.587	0.181	0.700	3.865	0.795
0.049	0.315	0.053	0.132	2.492	−0.038	0.153	0.620	0.206	0.767	3.728	0.827
0.062	0.374	0.072	0.213	2.963	0.184	0.176	0.657	0.237	0.837	3.526	0.855
0.076	0.425	0.092	0.306	3.345	0.362	1.000	1.000	1.000	1.000	1.000	0.000
0.092	0.476	0.115	0.411	3.585	0.499						
					70 °C						
0.000	0.000	0.000	0.000	1.005	−0.995	0.106	0.517	0.137	0.562	4.086	0.732
0.023	0.175	0.021	0.036	1.738	−0.444	0.122	0.557	0.161	0.655	4.063	0.801
0.035	0.246	0.035	0.078	2.212	−0.183	0.137	0.587	0.182	0.737	4.048	0.868
0.049	0.315	0.053	0.149	2.780	0.085	0.153	0.620	0.207	0.797	3.852	0.883
0.062	0.374	0.073	0.225	3.096	0.236	0.176	0.657	0.238	0.843	3.538	0.865
0.076	0.425	0.092	0.328	3.548	0.436	1.000	1.000	1.000	1.000	1.000	0.000
0.092	0.476	0.115	0.435	3.766	0.564						
					80 °C						
0.000	0.000	0.000	0.000	1.133	−0.875	0.106	0.517	0.138	0.598	4.317	0.810
0.023	0.175	0.021	0.042	1.980	−0.308	0.122	0.557	0.162	0.698	4.299	0.885
0.035	0.246	0.036	0.090	2.506	−0.049	0.137	0.587	0.183	0.771	4.206	0.929
0.049	0.315	0.054	0.163	3.015	0.176	0.153	0.620	0.208	0.805	3.872	0.896
0.062	0.374	0.074	0.255	3.468	0.369	0.176	0.657	0.239	0.846	3.534	0.868
0.076	0.425	0.093	0.353	3.781	0.515	1.000	1.000	1.000	1.000	1.000	0.000
0.092	0.476	0.116	0.466	4.004	0.645						
					90 °C						
0.000	0.000	0.000	0.000	1.269	−0.762	0.106	0.517	0.140	0.622	4.456	0.856
0.023	0.175	0.022	0.049	2.229	−0.185	0.122	0.557	0.163	0.727	4.445	0.936
0.035	0.246	0.037	0.010	2.728	0.043	0.137	0.587	0.184	0.766	4.154	0.915
0.049	0.315	0.055	0.175	3.190	0.241	0.153	0.620	0.209	0.809	3.866	0.898
0.062	0.374	0.074	0.273	3.664	0.435	0.176	0.657	0.241	0.841	3.493	0.852
0.076	0.425	0.094	0.378	4.009	0.588	1.000	1.000	1.000	1.000	1.000	0.000
0.092	0.476	0.117	0.501	4.265	0.729						
					100 °C						
0.000	0.000	0.000	0.000	1.412	−0.655	0.106	0.517	0.141	0.657	4.671	0.924
0.023	0.175	0.022	0.054	2.427	−0.095	0.122	0.557	0.165	0.735	4.462	0.946
0.035	0.246	0.037	0.110	2.946	0.127	0.137	0.587	0.186	0.768	4.137	0.913
0.049	0.315	0.056	0.193	3.466	0.335	0.153	0.620	0.210	0.840	3.469	0.846
0.062	0.374	0.075	0.297	3.943	0.523	0.176	0.657	0.242	0.840	3.469	0.846
0.076	0.425	0.095	0.399	4.186	0.644	1.000	1.000	1.000	1.000	1.000	0.000
0.092	0.476	0.119	0.530	4.469	0.792						
					110 °C						
0.000	0.000	0.000	0.000	1.559	−0.556	0.106	0.517	0.142	0.682	4.803	0.966
0.023	0.175	0.023	0.059	2.582	−0.030	0.122	0.557	0.166	0.735	4.427	0.940
0.035	0.246	0.038	0.121	3.184	0.212	0.137	0.587	0.187	0.768	4.106	0.907
0.049	0.315	0.057	0.210	3.715	0.415	0.153	0.620	0.212	0.785	3.705	0.840
0.062	0.374	0.076	0.317	4.147	0.585	0.176	0.657	0.244	0.836	3.432	0.833
0.076	0.425	0.096	0.434	4.504	0.737	1.000	1.000	1.000	1.000	1.000	0.000
0.092	0.476	0.120	0.561	4.684	0.857						
					120 °C						
0.000	0.000	0.000	0.000	1.712	−0.462	0.106	0.517	0.143	0.677	4.718	0.947
0.023	0.175	0.023	0.066	2.833	0.068	0.122	0.557	0.168	0.723	4.315	0.909
0.035	0.246	0.039	0.130	3.363	0.272	0.137	0.587	0.189	0.753	3.994	0.871
0.049	0.315	0.058	0.228	3.959	0.488	0.153	0.620	0.214	0.788	3.689	0.839
0.062	0.374	0.077	0.339	4.381	0.652	0.176	0.657	0.245	0.825	3.364	0.805
0.076	0.425	0.098	0.463	4.747	0.805	1.000	1.000	1.000	1.000	1.000	0.000
0.092	0.476	0.121	0.592	4.890	0.917						
					130 °C						
0.000	0.000	0.000	0.000	1.869	−0.374	0.106	0.517	0.145	0.656	4.525	0.895
0.023	0.175	0.024	0.070	2.940	0.108	0.122	0.557	0.169	0.704	4.162	0.862
0.035	0.246	0.039	0.142	3.604	0.348	0.137	0.587	0.190	0.738	3.881	0.833
0.049	0.315	0.059	0.242	4.143	0.541	0.153	0.620	0.215	0.769	3.572	0.793
0.062	0.374	0.079	0.354	4.498	0.686	0.176	0.657	0.247	0.813	3.293	0.774
0.076	0.425	0.099	0.479	4.849	0.834	1.000	1.000	1.000	1.000	1.000	0.000
0.092	0.476	0.122	0.612	4.994	0.949						

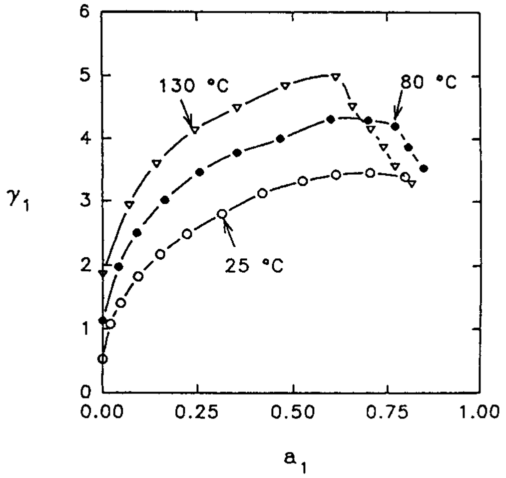

Figure 4. Activity coefficient of water in amorphous starch, γ_1, as a function of the water activity, a_1, at 25, 80, and 130 °C.

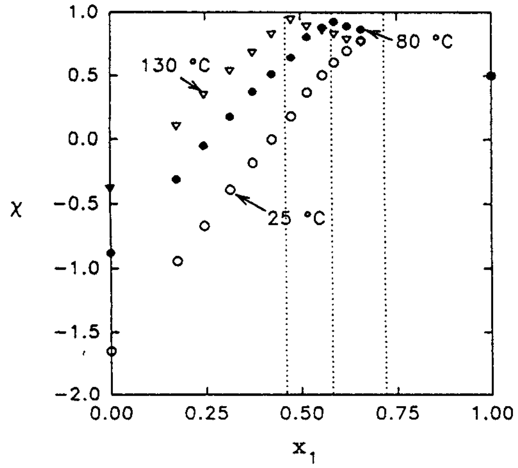

Figure 5. Concentration dependent van Laar heat of mixing, χ, of water in amorphous starch as a function of the molar water concentration, x_1, and glass transition points detected by calorimetry[22,38] denoted by a dashed line corresponding well with the maximum value of the excess functions at 80 and 130 °C.

Using the functions $\chi/V_1(1/T)$ represented in Figure 6, the cohesive energy density was estimated to be 1.21 GJ/m^3 at 25 °C for dry starch with eq 22. This value is comparable with the experimental 1.57 GJ/m^3 reported for cellulose using a similar approach[47] and is somewhat higher than the 0.78 GJ/m^3 estimated by atomistic modeling of amorphous starch.[48] The results are presented in Table 3 and the concentration dependence of the solubility parameter, δ, and of the cohesive energy density, ced$^{25°C}$, are plotted in Figure 7.

Data Analysis and Discussion

Freundlich−Flory Model of Sorption. The water sorption isotherms of amorphous starch were fitted with the explicit set of eqs 3, 5, and 7 using a Marquardt least-squares fit procedure. Table 4 and Figure 8 show the temperature behavior of the four adjustable parameters of eqs 5 and 7 and include values calculated for 5, 15, 35, 45, and 55 °C from the linear isosteres presented in Figure 2.

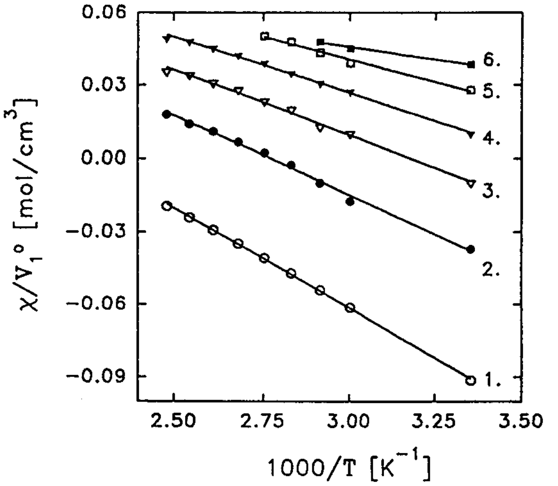

Figure 6. Linear relationships (regression coefficients $r > 0.999$) used to estimate the solubility parameter of amorphous starch containing (1) 0.005, (2) 0.035, (3) 0.062, (4) 0.92, (5) 0.122, and (6) 0.153 weight fraction of water.

Table 3. Solubility Parameter, δ, and Cohesive Energy Density at 25 °C, Ced$^{25°C}$, of Amorphous Starch Containing w_1 Weight Fraction of Water

w_1	δ (MPa$^{1/2}$)	ced$^{25°C}$ (GJ/m^3)
0.000	34.84	1.214
0.023	34.85	1.214
0.035	36.00	1.297
0.049	36.33	1.320
0.062	37.00	1.369
0.076	37.39	1.368
0.092	37.75	1.425
0.106	38.17	1.457
0.122	38.57	1.488
0.137	39.13	1.531
0.153	39.88	1.590
0.176	41.42	1.715
1.000	47.94[a]	2.298[a]

[a] Values taken from the Handbook of Polymers (1989).

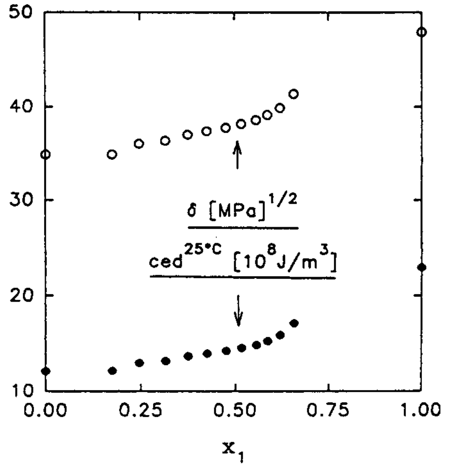

Figure 7. Solubility parameters δ and the cohesive energy densities, ced$^{25°C}$, of amorphous starch containing x_1 mole fraction of water.

The temperature dependence of f indicates a transition from a heterogeneous sorption ($f < 1$) to a homogeneous one ($f = 1$) at around 60 °C. This type of distribution of the adsorption energies has also been found by the molecular modeling of the same system.[48] To interpret the values obtained for q, it is useful to remember that the vibrational, rotational, and translational contributions to the molecular partition function, q, of pure water at 25 °C and atmospheric pressure are of the order of $q^V \approx 1$, $q^R \approx 43$, and $q^T \approx 3 \times 10^6$, respectively.[49] At 5 and 15 °C, the molecular partition

Table 4. Temperature Dependence of the Parameters Estimated from the Sorption Isotherms of Amorphous Starch with the Freundlich–Flory Sorption Model Eqs 3, 5, and 7 at Temperatures T

T (°C)	f ±0.01–0.15[b]	q ±0.1–0.3[b]	θ^0 ±0.01–0.03[b]	χ^∞ ±0.02–0.5[b]	$\langle \Delta a_1 \rangle$
5	0.48	1.00[a]	0.191	1.17	0.004
15	0.53	1.00[a]	0.190	1.18	0.004
25	0.68	2.39	0.135	1.10	0.004
35	0.63	2.08	0.126	1.10	0.006
45	0.69	2.84	0.105	1.08	0.004
55	0.76	3.83	0.088	1.08	0.003
60	0.87	7.38	0.069	1.04	0.004
70	1.00[a]	9.81	0.062	1.06	0.005
80	1.00[a]	11.0	0.052	1.06	0.004
90	1.00[a]	13.3	0.043	1.04	0.011
100	1.00[a]	17.8	0.035	1.02	0.016
110	1.00[a]	34.4	0.025	0.98	0.018
120	1.00[a]	126.5	0.018	0.95	0.021
130	1.00[a]	$1/q \rightarrow 0$	0.014	0.90	0.025

[a] Constrained Values (see also text). [b] Confidence Intervals. [c] $\langle \Delta a_1 \rangle$ = Average Deviation between Experimental and Calculated Water Activites.

function of the adsorbed water molecules reaches the lowest physically meaningful limit ($q \approx 1$), which characterizes water in ice, where all translations and rotations of the molecules are frozen. It is only above 100 °C that the value predicted for q corresponds to freely rotating molecules. A hindered mobility of water in starch was recently reported in an atomistic modeling study of the same system, where it was found that the correlation times of the rotations of water molecules that require a change in the direction of the dipole are much longer in starch than in pure water.[48] Anisotropic movements of water in starch were also observed by proton NMR measurements, which indicated a distribution of the mobility of water at the lowest water concentrations and a molecular mobility increasing gradually with the water content.[50,51]

χ^∞ predicts phase separation at values larger than 0.5 according to the Flory theory of solutions.[5,10,11,13] Therefore, the high values obtained suggest that φ_1^{Fl} is preferentially homocoordinated rather than heterocoordinated to the solid mixture composed of φ_1^{Fr} and φ_2, as is supported by the nature of the clustering functions presented below. In this sense, the decrease of χ^∞ with temperature indicates an increasing solubilization of starch in water. The values predicted for χ^∞ are comparable to the 1.4 measured at 25 °C by gas–liquid chromatography on hydroxypropylcellulose, a cellulose derivative in which the whole water behaves as φ_1^{Fl} in starch.[52–54]

The ratio θ^0 relating φ_1^{Fr} to φ_2 at saturated vapor pressure decreases asymptotically from 20% at 5 °C to 1% at 130 °C and can be expected to vanish as the experimental temperature approaches the glass transition temperature of the pure polymer. The temperature where $\theta^0 = 0$ and the Flory isotherm ($\chi^\infty \geq 0$) is recovered can be estimated to occur at 175 °C from the linear $\chi^\infty(1/T)$ function presented in Figure 1. However, the calorimetric results suggest that the glass-melt transition of dry starch is above 200 °C. Flory water sorption isotherms ($\chi^\infty \geq 0$) were reported for starch plasticized by more than 30 wt % glycerol[55] and for glucose glass at 25 °C.[56]

The sorption isotherm at 25 and 80 °C are shown in Figure 9 with the corresponding volume fractions, φ_1^{Fr} and φ_1^{Fl}, calculated using the numerical results presented in Table 3. The plasticization of starch by water can be interpreted by considering that an increase in the temperature at constant composition corresponds to a reduction of the relative proportion of less mobile φ_1^{Fr} and to an increase of the relative proportion of more mobile φ_1^{Fl}. The activity coefficients γ_1^{Fr} and γ_1^{Fl} calculated separately for the two water phases are plotted in Figure 10 at 25 and 80 °C with the experimental activity coefficients γ_1. It can be seen in Figure 10 that γ_1^{Fr} reflects all the thermodynamic properties found for water in starch glass ($\ln \gamma_1^\infty < 1$, $\partial\gamma_1/\partial a_1 > 0$, and $\partial\gamma_1/\partial T > 0$) and γ_1^{Fl} those found for water in starch melt ($\ln \gamma_1^\infty > 1$, $\partial\gamma_1/\partial a_1 < 0$, and $\partial\gamma_1/\partial T < 0$). The temperature dependence of the activity coefficient can be understood as follows. In an adsorption process, the strength of a water–starch contact is expected to be reduced on increasing the temperature. In a solubilization process, the breakage of the hydrogen bonds that keep starch strongly self-associated becomes easier as the temperature is increased.

Kirkwood Theory of Solutions. The excess functions, $\gamma_1(a_1)$ and $\chi\varphi_2^2(\varphi_2)$, used to calculate the clustering functions according to eqs 13 and 14 are shown in Figures 4 and 11. The self-clustering functions of water in amorphous starch, $G_{11}/\bar{v}_1$, are compared in Figure 12 with those calculated separately for φ_1^{Fr} and φ_1^{Fl}. Negative self-clustering functions of less than −1 are obtained for φ_1^{Fr}, indicating a preferential heterocoordination for the adsorbed molecules. Similar behaviors have been reported for other aqueous systems including collagen,[27] cellulose, cellulose acetate and ethylcellulose[54] and casein.[58,59] Positive self-clustering functions are obtained for φ_1^{Fl}, reflecting, as $\chi^\infty > 0.5$ in the Freundlich–Flory model, a clustering tendency or preferential homocoordination of the Flory water in starch.[27,57]

The positive values of $G_{11}/\bar{v}_1$ above the glass transition of starch are typical for plasticizers and suggest that one water molecule creates space to the next water molecule by swelling the polymer and by increasing its free volume. The negative values below −1 suggest that water molecules are separated from the next water molecule by several times their own volume. This follows the earlier observation according to which low concentrations of water have the effect of an antiplasticizer on starch glasses and result in an increase of its density and a decrease of its free volume.[38,66]

The self-clustering functions calculated for the total water content, $G_{11}/\bar{v}_1$, are plotted in Figure 13 at 25, 80, and 130 °C as a function of the molar concentration of water in starch. In the intermediate concentration range, the effect of temperature is not pronounced, but at a water concentration corresponding to the glass–melt transition of the system at a given experimental temperature, $G_{11}/\bar{v}_1$ values change sign and become positive. Depending on the temperature, two types of behavior can be observed as the polymer is diluted by water. The divergent self-clustering functions of water above the glass transitions reflect that the phase-separation tendency[60–62] of water molecules is enhanced between 25 and 80 °C. Above 80 °C, the self-clustering functions of water take finite values in melts, reflecting, presumably, the thermal disruption of the last hydrogen bonds keeping starch in a partial self-association.

Table 5. Clustering Functions $G_{11}/\bar{v}_1$, $G_{22}/\bar{v}_2$, and $G_{12}/\bar{v}_1 = G_{21}/\bar{v}_2$, as a Function of the Volume Fraction of Starch in the Mixture, φ_2, at 25, 60, 70, 80, 90, 100, 110, 120, and 130 °C[a]

φ_2	$\bar{v}_1$	$\bar{v}_2$	$G_{11}/\bar{v}_1$	$G_{22}/\bar{v}_2$	$G_{12}/\bar{v}_1 = G_{21}/\bar{v}_2$	φ_2	$\bar{v}_1$	$\bar{v}_2$	$G_{11}/\bar{v}_1$	$G_{22}/\bar{v}_2$	$G_{12}/\bar{v}_1 = G_{21}/\bar{v}_2$
25 °C											
1.000	6.232	108.3	−39.6	−1.00	1.00	0.866	14.82	105.6	−3.81	−1.13	0.65
0.981	10.01	107.9	−19.0	−1.02	0.65	0.842	15.74	104.6	−2.44	−1.19	0.73
0.967	11.34	107.5	−11.4	−1.03	0.64	0.822	16.05	104.2	−1.81	−1.22	0.82
0.949	12.51	107.1	−8.29	−1.05	0.61	0.797	16.36	103.7	−0.85	−1.26	1.04
0.930	13.43	106.6	−5.84	−1.08	0.64	0.765	16.68	103.2	1.72	−1.31	1.83
0.911	14.16	106.1	−4.62	−1.10	0.65	0.000	18.07	96.4	−1.00		1.00
0.888	14.82	105.6	−3.81	−1.13	0.65						
60 °C											
1.000	7.132	108.6	−32.5	−1.00	1.00	0.864	15.72	105.6	−2.66	−1.16	0.91
0.980	10.71	108.3	−15.9	−1.02	0.72	0.840	16.13	105.1	−2.01	−1.19	1.15
0.965	11.96	107.9	−10.6	−1.04	0.68	0.819	16.13	105.1	−2.01	−1.19	1.15
0.947	13.07	107.5	−7.49	−1.06	0.76	0.794	16.71	104.3	−0.43	−1.26	3.11
0.928	13.94	107.0	−5.74	−1.08	0.74	0.763	17.01	103.8	1.15	−1.31	4.04
0.908	14.63	106.6	−4.28	−1.10	0.76	0.000	18.33	97.48	−1.00		1.00
0.885	15.25	106.1	−3.37	−1.13	0.81						
70 °C											
1.000	7.424	108.7	−30.0	−1.00	1.00	0.986	15.87	105.8	−1.33	−1.16	0.95
0.979	10.94	108.4	−15.4	−1.02	0.69	0.839	16.27	105.3	−0.51	−1.19	1.09
0.965	12.17	108.0	−10.7	−1.04	0.64	0.818	16.56	104.9	0.47	−1.22	1.33
0.947	13.27	107.6	−7.12	−1.06	0.65	0.793	16.84	104.5	2.55	−1.26	1.93
0.927	14.12	107.2	−5.49	−1.08	0.65	0.762	17.14	104.0	16.9	−1.31	6.60
0.908	14.80	106.7	−4.12	−1.10	0.68	0.000	18.43	97.70	−1.00		1.00
0.885	15.41	106.2	−2.54	−1.13	0.80						
80 °C											
1.000	7.735	108.8	−29.1	−1.00	1.00	0.862	16.03	105.9	−1.79	−1.16	0.87
0.979	11.18	108.5	−14.9	−1.02	0.70	0.838	16.42	105.5	−0.64	−1.19	1.07
0.964	12.40	108.2	−10.4	−1.04	0.65	0.817	16.70	105.1	0.95	−1.22	1.44
0.946	13.47	107.8	−5.36	−1.06	0.75	0.792	16.98	104.7	6.34	−1.26	2.93
0.926	14.31	107.3	−4.37	−1.08	0.73	0.761	17.27	104.2	120.1	−1.31	39.3
0.907	14.98	106.9	−3.53	−1.10	0.74	0.000	18.55	98.02	−1.00		1.00
0.884	15.58	106.4	−2.65	−1.13	0.78						
90 °C											
1.000	8.066	109.0	−27.8	−1.00	1.00	0.860	16.20	106.1	−1.55	−1.16	0.91
0.978	11.45	108.6	−14.2	−1.02	0.71	0.837	16.59	105.7	−0.20	−1.20	1.16
0.963	12.64	108.3	−9.84	−1.04	0.66	0.816	16.87	105.3	6.20	−1.23	2.63
0.945	13.69	107.9	−5.30	−1.06	0.75	0.791	17.14	104.9	7.13	−1.26	3.15
0.926	14.52	107.5	−4.29	−1.08	0.74	0.759	17.42	104.4	8.77	−1.32	4.10
0.906	15.17	107.0	−3.42	−1.10	0.75	0.000	18.67	98.35	−1.00		1.00
0.883	15.76	106.6	−2.49	−1.13	0.80						
100 °C											
1.000	8.419	109.1	−26.5	−1.00	1.00	0.859	16.39	106.3	−1.50	−1.16	0.92
0.978	11.73	108.8	−13.6	−1.02	0.71	0.835	16.77	105.9	6.84	−1.20	2.55
0.963	12.90	108.5	−9.52	−1.04	0.67	0.814	17.04	105.5	7.39	−1.23	2.91
0.944	13.93	108.1	−5.12	−1.06	0.76	0.790	17.31	105.1	8.04	−1.27	3.41
0.925	14.74	107.6	−4.15	−1.08	0.74	0.758	17.59	104.6	8.79	−1.32	4.13
0.905	15.38	107.2	−3.31	−1.11	0.76	0.000	18.81	98.70	−1.00		1.00
0.881	15.95	106.7	−2.41	−1.13	0.81						
110 °C											
1.000	8.764	109.2	−25.3	−1.00	1.00	0.858	16.59	106.5	−0.62	−1.17	1.06
0.977	12.02	108.9	−13.1	−1.02	0.72	0.834	16.96	106.1	10.0	−1.20	3.20
0.962	13.17	108.6	−9.14	−1.04	0.68	0.813	17.23	105.7	9.76	−1.23	3.48
0.943	14.18	108.2	−5.20	−1.06	0.75	0.788	17.50	105.3	8.75	−1.27	3.62
0.924	14.97	107.8	−4.08	−1.08	0.75	0.756	17.77	104.8	6.62	−1.32	4.45
0.904	15.60	107.4	−3.10	−1.10	0.78	0.000	18.97	99.02	−1.00		1.00
0.880	16.17	106.9	−1.95	−1.14	0.87						
120 °C											
1.000	9.136	109.4	−23.9	−1.00	1.00	0.857	16.81	106.7	8.76	−1.17	2.45
0.977	12.33	109.1	−12.5	−1.02	0.73	0.832	17.17	106.3	8.65	−1.20	2.71
0.961	13.45	108.8	−8.74	−1.04	0.70	0.811	17.43	105.9	8.12	−1.23	2.87
0.942	14.45	108.4	−5.29	−1.06	0.77	0.786	17.70	105.5	6.97	−1.27	2.94
0.923	15.22	108.0	−3.98	−1.09	0.78	0.755	17.97	105.1	5.01	−1.33	2.81
0.902	15.84	107.6	−2.77	−1.11	0.82	0.000	19.14	99.37	−1.00		1.00
0.879	16.39	107.1	−1.19	−1.14	2.17						
130 °C											
1.000	9.523	109.5	−22.6	−1.00	1.00	0.855	17.04	106.9	7.54	−1.17	2.45
0.976	12.65	109.2	−11.9	−1.02	0.73	0.831	17.40	106.5	7.40	−1.20	2.71
0.961	13.76	108.9	−8.30	−1.04	0.70	0.810	17.66	106.2	6.97	−1.23	2.87
0.941	14.73	108.6	−4.67	−1.06	0.77	0.785	17.91	105.8	6.07	−1.27	2.94
0.921	15.49	108.2	−3.61	−1.09	0.78	0.753	18.17	105.3	4.51	−1.33	2.81
0.901	16.09	107.8	−2.64	−1.11	0.82	0.000	19.33	99.73	−1.00		1.00
0.878	16.63	107.3	7.39	−1.14	2.17						

[a] $\bar{v}_1$ and $\bar{v}_2$ are partial molar volumes of water and anhydroglucose, respectively.

The same tendencies are reflected by $-G_{12}/\bar{v}_1$ at 25 and 130 °C in Figure 14, where it can be seen that the affinity of water for starch is large in glasses and is depressed in melts where like molecules stay preferentially together. Figure 15 shows the volumes excluded by a water molecule placed next to an anhydroglucose unit ($-G_{12}$) and that excluded by an anhydroglucose unit placed next to a water molecule ($-G_{21}$). In the limit of

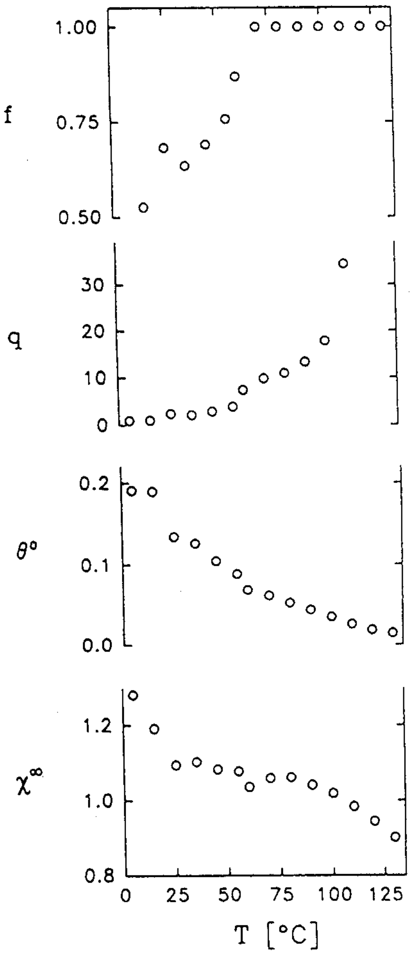

Figure 8. Temperature dependence of the parameters of eqs 5 and 7.

the pure components, the concentration fluctuations vanish and these integrals take the value of the corresponding partial molar volumes. $S^{\varphi}_{CC}(0)/\bar{v}_1$ is plotted at 25 and 130 °C in Figure 16 to show how the concentration fluctuations are frozen in glasses and become only important above the glass transition.

Conclusion

The sigmoidal water sorption isotherms are fitted to the explicit Freundlich–Flory model presented in this paper by assuming that the solvent of a polymer undergoing glass transition on dilution is partitioned over two phases. A low ice like molecular partition function is estimated for the Freudlich water adsorbed in polymer glasses at concentrations and temperatures where it has, according to the Kirkwood theory of solutions, the negative excluded volume of an antiplasticizer. This is also reflected in density increases and free volume reductions observed previously at low water concentrations. A large and positive van Laar heat of mixing indicating solvent clustering is predicted for the Flory water, showing, according to the Kirkwood theory of solutions, the positive excluded volumes of a plasticizer.

The clustering functions suggest further that the low mobility of starch below the glass transition prevents water molecules from replacing all the hydrogen bonds, keeping starch self-associated. The divergent clustering functions observed below 80 °C reflect a phase separation tendency of water molecules, and at higher temperatures, the opposite can be observed, as the clustering tendency of water in starch melts is depressed by an increase in temperature. At these high temperatures the mobility of starch molecules increases with increasing water content and allows eventually the remaining starch–starch hydrogen bonds to be replaced by starch–water hydrogen bonds, as has been shown by the atomistic modeling of this system. A transition to Flory sorption can be estimated by gas chromatography to occur at 175 °C. Below this temperature, the antiplasticizer properties of water in starch glass confer a sigmoidal shape to the sorption isotherms. The Freundlich–Flory sorption model provides a consistent description of the solvation, the swelling, and the dissolution of hydrophilic polymer glasses in a solvent like water, whereas the Brunauer–Emmet–Teller model is only physically meaningful for the adsorption of nonsolvents such as oxygen or nitrogen gases.

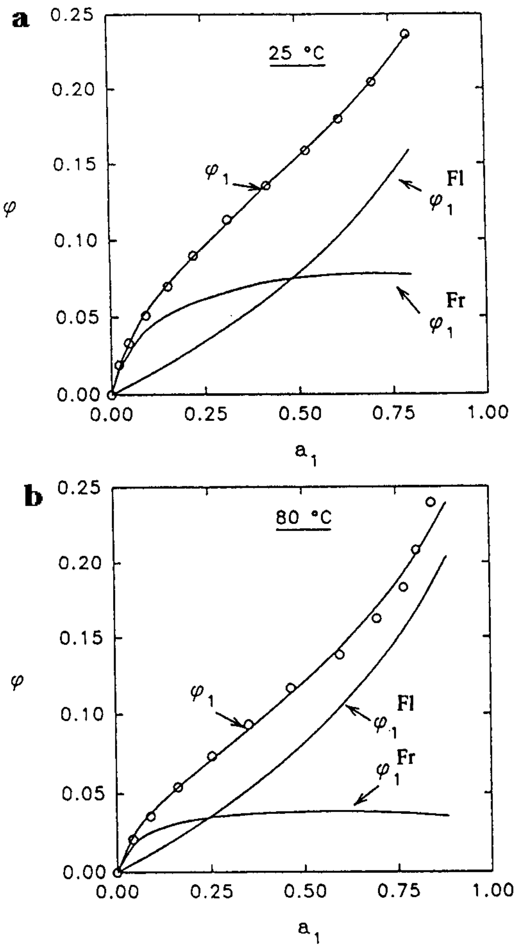

Figure 9. Experimental (symbols) and computed (line) water sorption isotherms of starch at 25 and 80 °C as well as the two water phases φ_1^{Fr} and φ_1^{Fl} corresponding to Freundlich and Flory isotherms, respectively.

Appendix I

With the Lagrange unknown multiplier method, the constant appearing in the generalized Freundlich equation[17,18] can be identified as the mean molecular partition function of the adsorbed gas (q).[20]

The adsorption of $N = \sum N_i$ gas molecules with energies ϵ_i at the $N^0 = \sum N^0_i$ sites of a heterogeneous

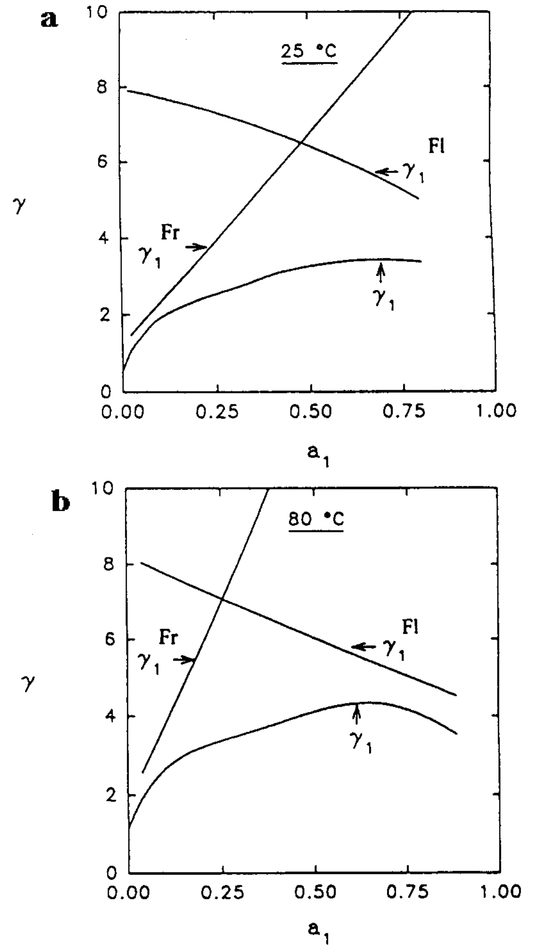

Figure 10. Activity coefficients, γ_1^{Fr} and γ_1^{Fl}, of the two water phases at 25 and 80 °C.

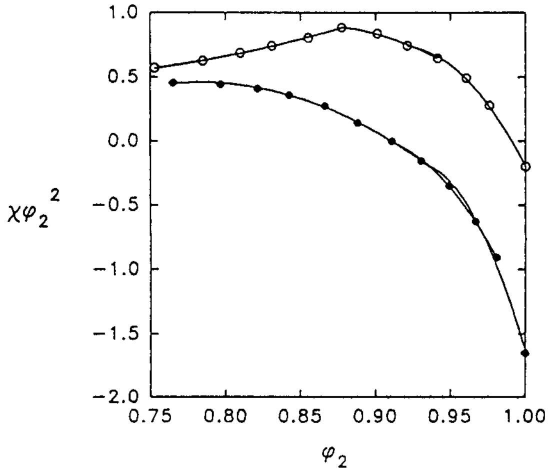

Figure 11. Excess functions $\chi\varphi_2^2(\varphi_2)$ at 25 °C (filled symbols) and 130 °C (open symbols) fitted by quadratic equations to calculate the cluster integrals with eq 14.

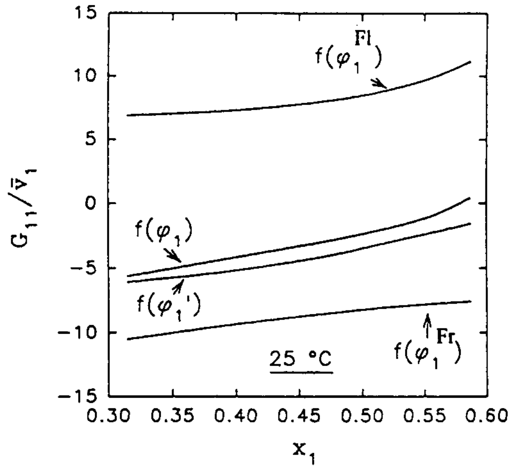

Figure 12. $G_{11}/\bar{v}_1$ clustering functions at 25 °C as a function of the molar concentration of water, x_1, in amorphous starch. Values calculated from the slope of the function $\chi\varphi_2^2(\varphi_2)$ are denoted by φ_1, φ_1^{Fr}, and φ_1^{Fl}, while those calculated for the total water content from the slope of the functions $\gamma_1(a_1)$ are denoted by φ_1'.

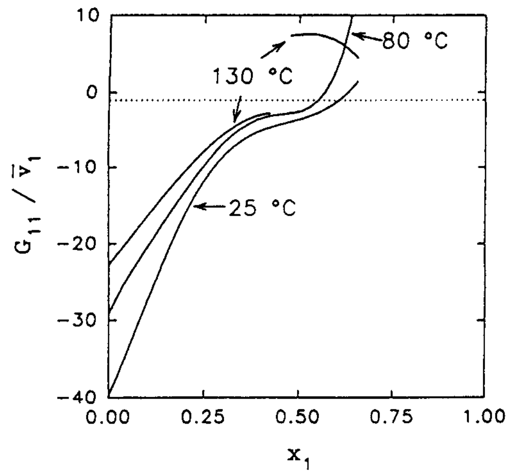

Figure 13. Clustering functions, $G_{11}/\bar{v}_1$, at 25, 80, and 130 °C as a function of the molar concentration of water, x_1, in amorphous starch. The dashed line represents the clustering function of an ideal solution of randomly arranged equal-sized molecules.

surface can, for $N < N^0$, be written[19]

$$Q(N,N^0,T) = \prod_i Q_{N_i} = \prod_i \frac{N^0_i!}{N_i!(N^0_i! - N_i)!} q^{\Sigma_i N_i} \exp(N_i\epsilon_i/kT) \quad \text{(A.1)}$$

where Q is the partition function given by the product of the Q_{N_i} contributions, q is the mean molecular partition function of the adsorbed molecules, k is the Boltzmann constant, and T is the temperature with the classical approximation $\ln Q_{(\max)} = \ln Q_{N_i}(\max)$, the partition function Q_{N_i}, giving the maximum value of Q, can be found with the Lagrange unknown multiplier, α, by defining

$$N_i = \frac{N_i^0}{(1/q)\exp(\alpha - \epsilon_i/kT) + 1} \quad \text{(A.2)}$$

The substitution of eq A.2 in eq A.1 gives

$$\ln Q_{\max} = \sum_i N_i^0 \left\{ \frac{\alpha}{(1/q)\exp(\alpha - \epsilon_i/kT) + 1} - \ln\left[\frac{(1/q)\exp(\alpha - \epsilon_i/kT)}{(1/q)\exp(\alpha - \epsilon_i/kT) + 1}\right] \right\} \quad \text{(A.3)}$$

The undetermined multiplier, α, is obtained from the derivatives of the logarithmic partition function, ln Q,

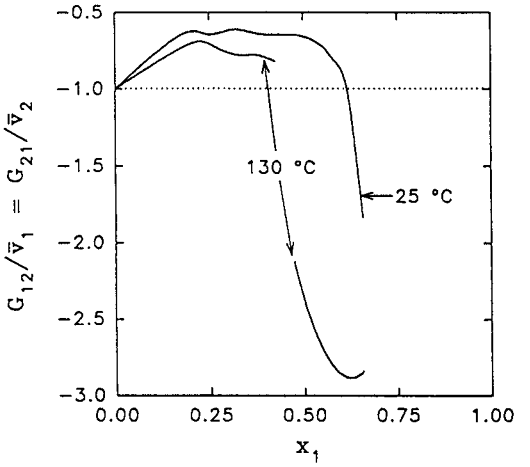

Figure 14. Clustering functions, $G_{12}/\bar{v}_1$, at 25 and 130 °C as a function of the molar concentration of water, x_1, in amorphous starch. The dashed line represents the clustering function of an ideal solution of randomly arranged equal-sized molecules.

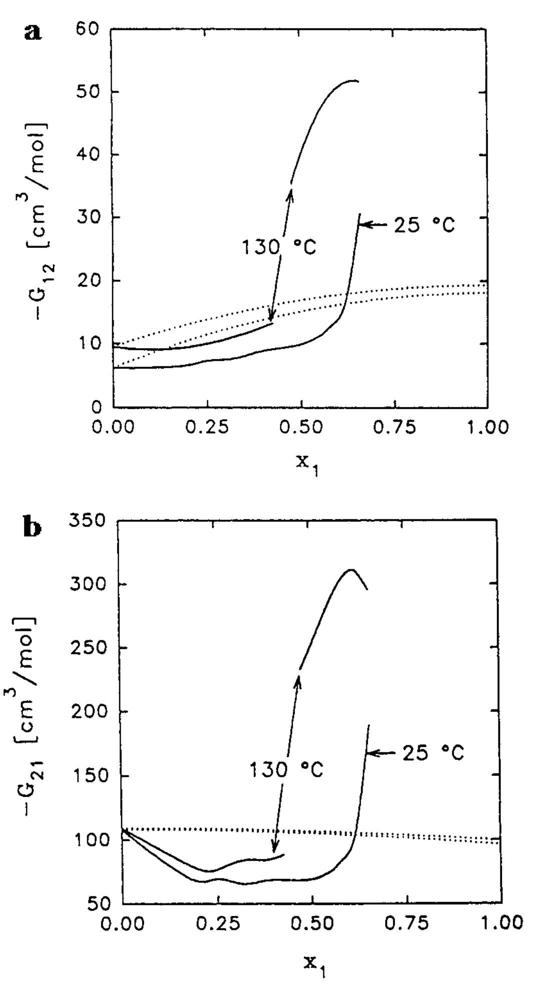

Figure 15. Cluster integrals, $-G_{12}$, and $-G_{21}$, at 25 and 130 °C as a function of the molar concentration of water, x_1, in amorphous starch. In the limit of the pure component where the concentration fluctuations vanish, G_{12} and G_{21} take the value of the corresponding partial molar volume represented here with dashed lines.

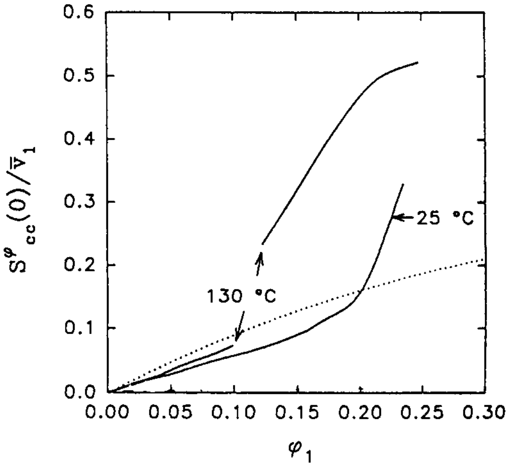

Figure 16. Reduced volume fraction related concentration fluctuation $S^{\varphi}_{CC}(0)/\bar{v}_1$ as a function of the volume fraction of water, φ_1, in amorphous starch. The dashed line represents the product $\varphi_1\varphi_2$ at 25 °C calculated for an ideal solution.

with respect to N

$$\mathrm{a} = \left(\frac{\partial \ln Q}{\partial N}\right)_{N^0,T} = -\left[\frac{\partial (A/kT)}{\partial N}\right]_{N^0,T} = -\frac{\Delta\mu}{kT} = -\ln a \qquad \text{(A.4)}$$

where ΔA is the Helmoltz free energy of mixing, $\Delta\mu$ and a are the chemical potential and the corresponding thermodynamic activity of the adsorbed gas molecules. The adsorption isotherm according to eq A.3 and eq A.4 is

$$N = \sum_i \frac{N_i^0}{(1/q)\exp[-(\Delta\mu + \epsilon_i)/kT] + 1} = \sum_i \frac{N_i^0}{(1/a)(1/q)\exp(-\epsilon_i/kT) + 1} \qquad \text{(A.5)}$$

and the generalized Freundlich equation is obtained on replacing the sum by the corresponding integral extending over $0 < \epsilon < +\infty$

$$\frac{N}{N^0}(p) = \int_0^{\infty} \frac{N^0(\epsilon)\,\mathrm{d}\epsilon}{1/(aq)\exp(-\epsilon/kT) + 1} \qquad \text{(A.6)}$$

where $N^0(\epsilon)$ gives the fraction of sites with an adsorption energy between ϵ and $\epsilon + \mathrm{d}\epsilon$. To deduce the partition of the adsorption energies from an isotherm, the function $N(\epsilon)$ must be solved to give N/N^0 as a function of the pressure, p. According to Sips, the simplest mathematical form able to fulfill the two physical boundary conditions $N/N^0(0) = 0$ and $N/N^0(\infty) = 1$ is given by eq 5 of this article.[17,18]

Appendix II

The sorption model proposed originally by Tomka combines the generalized Freundlich and Flory approaches into the following transcendental set of equations

$$a_1 = \varphi_1^{\mathrm{Fl}} \exp[(1 - \varphi_1^{\mathrm{Fl}}) + \chi^{\infty}\varphi_2(1 - \varphi_1^{\mathrm{Fl}})] \qquad \text{(A.7a)}$$

$$\chi^{\infty}(\varphi_2) - 1 + \ln\left[\frac{(\varphi_1^{\mathrm{Fr}})^{1/f}}{(\theta^0\varphi_2)^{1/f} - (\varphi_1^{\mathrm{Fr}})^{1/f}}\,\frac{1}{\mathrm{q}}\right] = \ln(\varphi_1^{\mathrm{Fr}}) \qquad \text{(A.7b)}$$

In eq A.7a,b χ^{∞} refers clearly to the change in the potential energy of a solvent molecule as it is transferred from the pure solvent in the pure polymer ($N_1 \rightarrow N_2$).[20,21] In eqs 6 and 7 of this paper, χ^{∞} concerns strictly the transfer of Flory solvent from the pure solvent in a solid mixture of the polymer and of the Freundlich solvent adsorbed according to eq 5 of this paper ($N_1^{\mathrm{Fl}} \rightarrow N_1^{\mathrm{Fr}} + N_2$).[22]

Acknowledgment. We gratefully acknowledge support by Grant No. 20-34058.92 of the Swiss National Fund for Scientific Research. We are also grateful to Prof. G. Vàncsó and Dr. J. Zhanjie Tan from the Chemistry Department of the University of Toronto where the chromatographic experiments were performed.

References and Notes

(1) Brunauer, S.; Emmet, P. H.; Teller, E. *J. Am. Chem. Soc.* **1938**, *60*, 309−319.
(2) Benson, S. W.; Ellis, D. A. *J. Am. Chem. Soc.* **1948**, *70*, 3563−3569.
(3) Benson, S. W.; Ellis, D. A.; Zwanzig, W. *J. Am. Chem. Soc.* **1950**, *72*, 2095−2105.
(4) Benson, S. W.; Seehof, J. M. *J. Am. Chem. Soc.* **1951**, *73*, 5053−5058.
(5) Rickles, R. N. *Ind. Eng. Chem.* **1966**, *58* (6), 19−35.
(6) Naylor T. V. In *Comprehensive Polymer Science*; Booth, C., and Price, C., Eds., Pergamon Press: Oxford, U.K., 1989; Vol. 2.
(7) Michaels, A. S.; Vieth, W. R.; Barrie J. A. *J. Appl. Phys.* **1963**, *34*, 13−22.
(8) Vieth, W. R.; Howell, J. M.; Hsieh, J. H. *J. Membr. Sci.* **1976**, *1*, 177−221.
(9) Paul, D. R.; Kemp, D. R. *ACS Symp. Ser.* **1985**, *285*, 253−275.
(10) Flory, P. J. *Principles of Polymer Chemistry*; Cornell University Press: Ithaca, New York, 1953.
(11) Flory, P. J. *Trans. Faraday Soc.* **1970**, *49*, 7−29.
(12) Huggins, M. L. *J. Chem. Phys.* **1942**, *9*, 440−445.
(13) Guggenheim, E. A. *Mixtures*; Oxford University Press: Oxford, U.K., 1952.
(14) Van den Berg, C. Dissertation, Agricultural University of Wageningen, 1981.
(15) Hill, T. L.; Rowen, J. W. *J. Polym. Sci.* **1952**, 9, 93−95.
(16) Rowen, J. W. *J. Polym. Sci.* **1958**, *31*, 199−202.
(17) Sips, R. *J. Chem. Phys.* **1948**, *16* (5), 490−495.
(18) Sips, R. *J. Chem. Phys.* **1950**, *18* (8), 1024−1026.
(19) Hill, T. *Statistical Mechanics*; McGraw-Hill: New York, 1956.
(20) Tomka, I. Dissertation, University of Bern, 1973.
(21) Gàl, S.; Tomka, I.; Signer, R. *Chimia* **1976**, *30*, 65−68.
(22) Benczédi, D. ETH Dissertation No. 11203, Zurich, 1995.
(23) Kirkwood, J. G.; Buff, P. F. *J. Chem. Phys.* **1951**, *19*, 774−777.
(24) Zimm, B. H. *J. Phys. Chem.* **1953**, *21*, 934−935.
(25) Patterson, D. *Macromolecules* **1969**, *2*, 672−677.
(26) Patterson, D.; Tewari, Y. B.; Schreiber, H. P.; Guillet, J. E. *Macromolecules* **1971**, *4*, 356−359.
(27) Zimm, B. H.; Lundberg, J. L. *J. Phys. Chem.* **1956**, *60*, 425−428.
(28) Crank, J.; Park, G. S. *Diffusion in Polymers*; Academic Press: London, 1968.
(29) Chialvo, A. In *Fluctuation Theory of Mixtures*; Matteoli, E., Mansoori, G. A., Eds.; Taylor and Francis: New York, 1990.
(30) Berens, A. R. *Angew. Makromol. Chem.* **1975**, *47*, 97−110.
(31) Panayiotou, C. G.; Sanchez I. C. *J. Phys. Chem.* **1991**, *95*, 10090, 10097.
(32) Lundberg, J. L. *Pure Appl. Chem.* **1972**, *31*, 261−281.
(33) Bathia, A. B.; Thornton, D. E. *Phys. Rev. B* **1970**, *2* (8), 3004−3012.
(34) Horta, A. *Macromolecules* **1992**, *25*, 5651−5658.
(35) Curro, J. G.; Schweizer, K. S. *Macromolecules* **1991**, *24*, 6736−6747.
(36) Sanchez, I. C. *Macromolecules* **1990**, *24*, 908−916.
(37) Lipson, J. E. G.; Guillet, J. E. *Solubilities and Solubility Parameters from Inverse Gas Chromatography*; Pergamon Press: New York, 1982.
(38) Benczédi, D.; Tomka, I.; Escher, F. *Macromolecules* **1998**, *31*, 3055.
(39) Ashworth, A.; Price, G. J. *Macromolecules* **1986**, *12*, 358−361.
(40) Price, G. J.; Guillet, J. E. *J. Solution Chem.* **1987**, 16(6), 605−613.
(41) Conder, J. R.; Young, C. L. *Physico-Chemical Measurements by Gas Chromatography*; Wiley: Chichester, U.K., 1979.
(42) Newman, R. D.; Prausnitz, J. M. *AIChE J.* **1973**, *19* (4), 704−710.
(43) Gàl, S. *Die Methodik der Wasserdampf-Sorptionsmessungen*; Springer-Verlag: Berlin, 1967.
(44) Rouse, P. E. *J. Am. Chem. Soc.* **1947**, *69*, 1068−1073.
(45) Fish, B. P. *London Soc. Chem. Ind.* **1958**, 143−157.
(46) DiPaola-Baranyi, G.; Guillet, G. E. *Macromolecules* **1978**, *11*, 1, 228−235.
(47) Shvarts, A. G. *Kolloid Z.* **1956**, *18*, 753−759.
(48) Trommsdorff, U. R.; Tomka, I. *Macromolecules* **1995**, *28*, *8* (18), 6128−6150.
(49) Atkins, P. W. *Physical Chemistry*; Oxford University Press: Oxford, U.K., 1994.
(50) Tanner, S. F.; Hills, B. P.; Parker, R. *J. Chem. Soc., Faraday. Trans.* **1991**, *87*, 2613−2621.
(51) Roosen, G. A. Dissertation, Hamburg, **1991**.
(52) Aspler, J. S.; Gray, D. G. *Macromolecules* **1979**, *12*, 2, 562−566.
(53) Aspler, J. S.; Gray, D. G. *Macromolecules* **1981**, *14*, 1546−1549.
(54) Aspler, J. S.; Gray, D. G. *J. Polym. Sci.* **1983**, *21*, 1675−1689.
(55) Sala, R.; Tomka, I. *Angew. Makromol. Chem.* **1992**, *199*, 45−63.
(56) Kargin, V. A. *J. Polym. Sci.* **1957**, *23*, 47−55.
(57) Saeki, S.; Tsubokawa, M.; Yamaguchi, T. *Macromolecules* **1987**, *20*, 2930−2934.
(58) Tomka I. *Polymer Preprints* **1986**, *27* (2), 129−131.
(59) Kato, T. In *Fluctuation Theory of Mixtures*; Matteoli, E., Mansoori, G. A., Eds.; Taylor and Francis: New York, 1990.
(60) Rubio, G. R.; Patterson, D. *Fluctuation Theory of Mixtures*; Matteoli, E., Mansoori, G. A., Eds.; Taylor and Francis: New York, 1990.
(61) Nishikawa, K.; Kodera, Y.; Iijima, T. *J. Phys. Chem.* **1987**, *91*, 3694−3699.
(62) Nishikawa, K.; Hayashi, H.; Iijima, T. *J. Phys. Chem.* **1989**, *93*, 6559−6565.
(63) Beck, M. I.; Tomka, I. *Macromolecules* **1996**, *29* (7), 8759−8769.
(64) Beck, M. I.; Tomka, I. *J. Macromol. Sci., Phys. B* **1997**, *36* (1), 19−39.
(65) Beck, M. I.; Tomka, I. *J. Polym. Sci., Part B* **1996**, *35*, 639−653.
(66) Maeda, Y.; Paul, D. R. *J. Polym. Sci., Part B* **1987**, *25*, 1005−1016.

MA960950Y